Received: 2 November 2021 | Revised: 21 April 2022 | Accepted: 9 May 2022

DOI: 10.1002/eap.2700

ECOLOGICAL APPLICATIONS
ECOLOGICAL SOCIETY OF AMERICA

ARTICLE

Modeling impacts of drought-induced salinity intrusion on carbon dynamics in tidal freshwater forested wetlands

Hongqing Wang[1] | **Zhaohua Dai**[2,3] | **Carl C. Trettin**[2] | **Ken W. Krauss**[4] | **Gregory B. Noe**[5] | **Andrew J. Burton**[3] | **Camille L. Stagg**[4] | **Eric J. Ward**[4]

[1]U.S. Geological Survey, Wetland and Aquatic Research Center, Baton Rouge, Louisiana, USA

[2]Center for Forested Wetlands Research, USDA Forest Service, Cordesville, South Carolina, USA

[3]Michigan Technological University, College of Forest Resources and Environmental Science, Houghton, Michigan, USA

[4]U.S. Geological Survey, Wetland and Aquatic Research Center, Lafayette, Louisiana, USA

[5]U.S. Geological Survey, Florence Bascom Geoscience Center, Reston, Virginia, USA

Correspondence
Hongqing Wang
Email: wangh@usgs.gov

Funding information
NASA Carbon Monitoring Systems program, Grant/Award Number: 80HQTR18T0012; U.S. Geological Survey Climate Research and Development Program; U.S. Geological Survey Ecosystems Mission Area

Handling Editor: Stephen B. Baines

Abstract

Tidal freshwater forested wetlands (TFFW) provide critical ecosystem services including an essential habitat for a variety of wildlife species and significant carbon sinks for atmospheric carbon dioxide. However, large uncertainties remain concerning the impacts of climate change on the magnitude and variability of carbon fluxes and storage across a range of TFFW. In this study, we developed a process-driven Tidal Freshwater Wetlands DeNitrification-DeComposition model (TFW-DNDC) that has integrated new features, such as soil salinity effects on plant productivity and soil organic matter decomposition to explore carbon dynamics in the TFFW in response to drought-induced saltwater intrusion. Eight sites along the floodplains of the Waccamaw River (USA) and the Savannah River (USA) were selected to represent the TFFW transition from healthy to moderately and highly salt-impacted forests, and eventually to oligohaline marshes. The TFW-DNDC was calibrated and validated using field observed annual litterfall, stem growth, root growth, soil heterotrophic respiration, and soil organic carbon storage. Analyses indicate that plant productivity and soil carbon sequestration in TFFW could change substantially in response to increased soil pore water salinity and reduced soil water table due to drought, but in interactive ways dependent on the river simulated. These responses are variable due to nonlinear relationships between carbon cycling processes and environmental drivers. Plant productivity, plant respiration, soil organic carbon sequestration rate, and storage in the highly salt-impacted forest sites decreased significantly under drought conditions compared with normal conditions. Considering the high likelihood of healthy and moderately salt-impacted forests becoming highly salt-impacted forests under future climate change and sea-level rise, it is very likely that the TFFW will lose their capacity as carbon sinks without up-slope migration.

KEYWORDS
carbon storage and fluxes, DeNitrification-DeComposition (DNDC) model, drought, saltwater intrusion, soil salinity, soil water level

INTRODUCTION

Tidal freshwater forested wetlands (TFFW) play an important role in sequestering and storing atmospheric carbon (e.g., Krauss et al., 2018), therefore helping to mitigate some impacts of climate change. However, global accounting efforts focusing on "blue carbon" ecosystems often omit critical contributions from TFFW, including the carbon that is sequestered by TFFW in the biomass of plants and soils, losses of carbon via emissions of methane (CH_4) and carbon dioxide (CO_2) from plant and soil respiration, and exports of dissolved organic carbon (DOC), dissolved inorganic carbon (DIC), and particulate organic carbon (POC) to adjacent estuaries. Recent progress has been made to recognize these wetlands as significant blue carbon ecosystems (Lovelock & Duarte, 2019). It is important to account for the impacts of climate change on ecosystem transition and the consequences to carbon cycling to improve estimates of carbon balance in TFFW and their contribution to the overall global carbon budget. The location and low-lying position of TFFW make them especially vulnerable to saltwater intrusion from climate change-induced sea-level rise (SLR), drought, and increased frequency and extent of storm surges that affect tidal range and salinity along many rivers (Neubauer et al., 2013; Noe et al., 2013; Pierfelice et al., 2015; Thomas et al., 2015). The changes in salinity and hydroperiod due to climate change, major drivers of carbon storage and fluxes in upper estuaries (Krauss et al., 2018), need to be considered in carbon (C) budgeting efforts within coastal landscapes.

Soil moisture regime (or hydroperiod) is a key factor that regulates carbon balance and greenhouse gas (GHG) emissions in coastal wetlands, including the TFFW, because moisture affects soil oxygen availability, which affects plant growth (Conner et al., 2014) and major biogeochemical processes such as soil organic matter decomposition, nitrogen, and phosphorus mineralization, methanogenesis, nitrification and denitrification (Drexler et al., 2013; Korol & Noe, 2020; Krauss et al., 2012; Noe et al., 2013; Stagg et al., 2017). For example, continuous flooding influences on the growth of baldcypress (*Taxodium distichum*), a prominent TFFW species, vary from inconsequential to negative (e.g., review by Conner et al., 2014), depending on relative soil oxygen state. Flooding and oxygen availability have important impacts on soil CO_2 fluxes as well, with variable results depending on flood duration and frequency. Field studies and mesocosm experiments found that soil CO_2 fluxes were significantly lower under permanent flooding than under dry conditions in tidal swamps as a result of lower microbial biomass, low CO_2 production with anaerobiosis, and barriers to CO_2 diffusion through the water column (Krauss et al., 2012). Tidally flooded treatments sometimes contributed to higher soil CO_2 efflux rates from soil and live belowground root respiration (Krauss et al., 2012). Nevertheless, Liu et al. (2017) found that there was no significant increase in soil CO_2 emissions under flooding compared with wet–dry treatments.

Soil pore water salinity is another critical factor that affects plant growth, mortality, respiration, soil organic matter decomposition, methanogenesis, methanotroph community density, nitrogen, and phosphorus mineralization, nitrification, denitrification, and other processes in tidal wetlands (Cormier et al., 2013; Dai et al., 2018a; Krauss et al., 2009, 2012; Noe et al., 2013; Stagg et al., 2017; Weston et al., 2006). TFFW swamps typically persist only when salinity is less than two practical salinity units (psu). Increased soil salinity exceeding 2 psu is a critical threshold for TFFW (Hackney et al., 2007) that can be caused by drought, storm surge, and SLR, resulting in significant changes in forest community composition and structure from a mixture of multiple woody species to only a few species as marsh species invade (Liu et al., 2017; Noe et al., 2013; Pierfelice et al., 2015; Thomas et al., 2015). Leaf nitrogen (N) content also decreased and foliar C/N ratio increased with elevated soil salinity in TFFW along two south Atlantic coast rivers (Cormier et al., 2013). Therefore, the long-term impacts of increased salinity can cause massive plant community shifts, and concomitant changes in carbon source or litter quality that affect organic matter decomposition and soil mineralization (Stagg et al., 2017). Elevated soil salinity can even shift microbial mineralization pathways from methanogenesis to more energy-efficient iron reduction and sulfate reduction (Weston et al., 2006). Soil organic matter decomposition is often lowest at intermediate salinity ranges due to the simultaneous iron inhibition of methanogens and electron acceptor limitation of sulfate-reducing bacteria (Stagg et al., 2017).

To advance the understanding of the impacts of rising sea levels, the combined effects of increasing soil salinity and inundation on biogeochemical processes have been studied in field and laboratory/mesocosm experiments but have led to inconsistent outcomes (Krauss et al., 2012; Krauss & Whitbeck, 2012; Liu et al., 2017; Marton et al., 2012; Neubauer et al., 2013; Weston et al., 2011). Simulation tools (models) are effective at properly evaluating cause and effect in ecosystems to more fully understand dynamic processes and to guide implementation of management action (Dai et al., 2018b; Li et al., 2004; Stagg et al., 2017; Zhang et al., 2002). Currently available models either focus on terrestrial (e.g., nontidal) freshwater wetlands (e.g., Li et al., 2000, 2004) or mangroves (Dai et al., 2018a). In this research, our objectives were to: (1) develop a carbon and nitrogen process-driven biogeochemistry model for TFFW; (2) calibrate and validate the biogeochemistry model using field data; and (3) predict the impacts of coastal drought-induced salinity increase on aboveground and belowground carbon sequestration (the process of taking carbon from the atmosphere) and storage (the amount of carbon stored) at TFFW sites that are undergoing SLR.

MATERIALS AND METHODS

Study sites

The tidal freshwater forested wetland sites in this study are located along the coastal floodplains of the Waccamaw River, a blackwater river in South Carolina, and the Savannah River, an alluvial river in Georgia (Figure 1). Four sites along each river were selected based on increasing soil pore water salinity concentrations: tidal freshwater forests (upper, 0.1 psu), moderately salt-impacted forests at the freshwater–oligohaline transition (middle, 1.2–1.4 psu), highly salt-impacted forests (lower, 2.4–4.3 psu), and oligohaline marshes (marsh, 3.1–4.9 psu) (Krauss et al., 2018). This region has a humid climate with hot summers and mild winters: mean annual rainfall ranges from 92 to 152 cm and annual temperature averages 17.4°C with a maximum annual mean of 18.5°C and a minimum mean of 16.6°C during 1985–2014 (Thomas et al., 2015). Tides are semidiurnal on the Waccamaw and Savannah rivers, and tidal ranges at the river mouths are 1.1 and 2.3 m, respectively (Cormier et al., 2013; Krauss et al., 2018). The dominant tree species at upper sites include *T. distichum* (baldcypress), *Nyssa aquatica* (water tupelo), *Nyssa biflora* (swamp tupelo), *Acer rubrum* (red maple), and *Fraxinus* spp. (ash), whereas *T. distichum*, and *N. biflora* are dominant at middle sites, and *T. distichum* is dominant at lower sites. At the marsh sites, dominant species include *Zizaniopsis miliacea* (giant cutgrass), *Spartina cynosuroides* (big cordgrass), *Bolboschoenus robustus* (sturdy bulrush), and *Typha latifolia* (cattail) (Ensign et al., 2013). Marsh species are also actively encroaching into lower sites. Soils at these TFFW sites were assigned to the Typic Hydraquent family in the soil survey geographic database (SSURGO).

Modeling approach

We developed a process-driven biogeochemistry model for simulating carbon sequestration, export, and GHG emissions in TFFW and oligohaline marsh. The model is based on the mangrove version of the DeNitrification-DeComposition (DNDC) model (mangrove carbon assessment tool [MCAT], Dai et al., 2018a) with necessary modifications to meet the structural and functional requirements of TFFW. From this point forward, this biogeochemistry model is named the Tidal Freshwater Wetlands DNDC model (TFW-DNDC) to embrace the varied community types (from forest to oligohaline marsh) that exist along the salinity gradient. MCAT-DNDC is a process-based mangrove wetland biogeochemistry model in support of mangrove carbon assessment (Dai et al., 2018a, 2018b). It was developed by integrating biogeochemical processes of Forest-DNDC (Li et al., 2000) and wetland-DNDC (Li et al., 2004; Zhang et al., 2002), which accommodated freshwater wetland biogeochemistry, with new provisions for carbon, nitrogen, and phosphorus processing to incorporate changes in biogeochemical reactions mediated by nutrients, water level, salinity stress, and disturbance regimes (Dai et al., 2018a). MCAT-DNDC is among the first wetland biogeochemistry models that estimates carbon, nitrogen, and phosphorus dynamics in saline wetlands. It predicts mangrove growth including gross primary productivity (GPP) and net primary productivity (NPP), carbon accumulation in aboveground and belowground biomass, litter production, organic matter decomposition, and organic carbon (OC) accumulation in soil/sediment, and emissions of CO_2, CH_4, N_2O from soil surface and leaching of DIC, DOC, and POC, as well as the effects of nitrogen and phosphorus deficit and salt stress (salinity) on primary productivity, soil organic matter decomposition, and gas emissions (Dai et al., 2018a, 2018b). It can simulate carbon cycle response in mangroves to climate change, SLR, and other natural and anthropogenic disturbances (e.g., storms, fires, and harvesting) (Dai et al., 2018b).

The model structure, including the biophysical processes and stressors of TFW-DNDC, is shown in Figure 2. The ecological drivers of TFW-DNDC include climate, hydrology, soil, vegetation, and disturbance. TFW-DNDC consists of five submodels: hydrology, plant growth, soil organic matter, methanogenesis/methanotroph, and nitrification/denitrification in TFW-DNDC (Figure 2). The hydrology submodel describes hydrological processes such as evapotranspiration and factors that affect water level and soil salinity. The plant growth submodel determines gross and NPP, plant respiration, and carbon allocation into leaf, wood/stem, and root. The soil organic matter submodel describes three litter pools (very labile, labile, and resistant) and three soil organic matter pools (mineral carbon/microbe pool, humus pool, and passive pool) that have different C/N ratios and specific decomposition rates. The methanogenesis/methanotrophy submodel specifies the production of methane and consumption via methanogenesis and methanotrophy, respectively, as well as the effects of DOC, DIC, sulfate, nitrite, and

FIGURE 1 Location of the tidal freshwater forested wetlands (TFFW) and oligohaline marsh sites along the (a) Waccamaw River, South Carolina (SC), and (b) Savannah River, Georgia (GA) (USA).

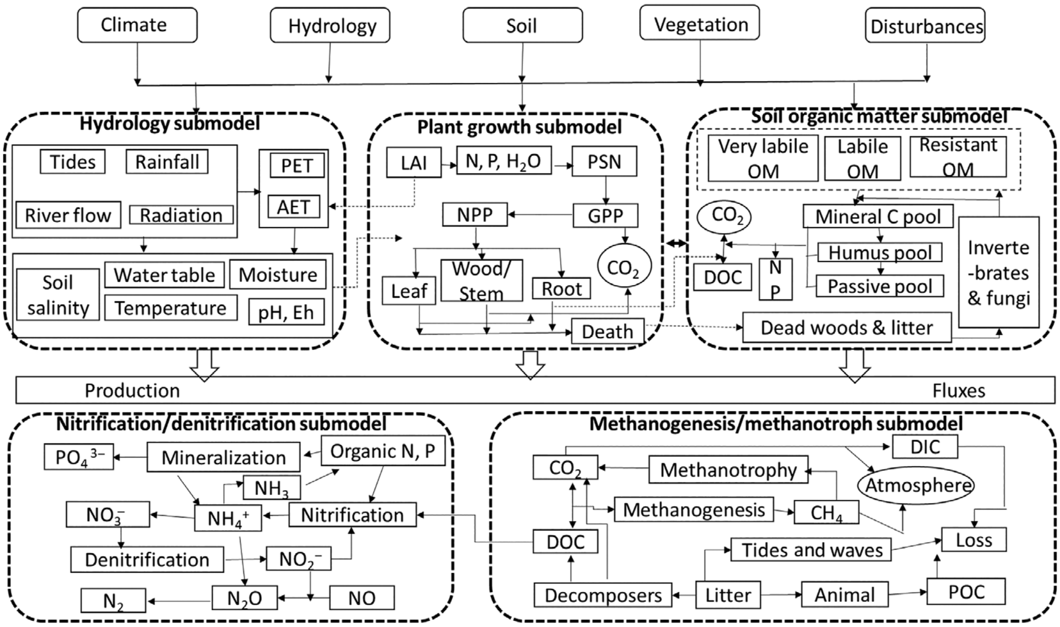

FIGURE 2 Diagram of the tidal freshwater forested wetlands (TFFW) BGC model modified from the mangrove carbon assessment tool-DeNitrification-DeComposition (MCAT-DNDC) model (Dai et al., 2018a). AET, actual evapotranspiration; DIC, dissolved inorganic carbon; DOC, dissolved organic carbon; Eh, redox potential; GPP, gross primary productivity; LAI, leaf area index; NPP, net primary productivity; OM, organic matter; PET, potential evapotranspiration; POC, particulate organic carbon; PSN, photosynthesis.

nitrate. The nitrification/denitrification submodel specifies the biogeochemical reactions including mineralization, nitrification, and denitrification that determine the production of N_2O, NO, and N_2. Specific soil environmental factors affecting soil organic matter decomposition, nitrification, denitrification, methanogenesis, and methanotroph include soil salinity, water level (moisture), redox potential, temperature, pH, and concentrations of substrates (NH_4^+, NO_3^-, DOC). The major biophysical processes and controlling factors in TFW-DNDC as inherited from MCAT-DNDC, Forest-DNDC, and wetland-DNDC are summarized in Appendix S1: Table S1. For details about the specific equations that describe these processes, refer to Dai et al. (2018a), Li et al. (2000), and Zhang et al. (2002). For this study, a 2-year spin-up period was adopted after model tests to reduce the influences of initial conditions and numerical calculations on model stability (carbon pools). Soil depth was simulated to 50 cm below the soil surface.

In this study, the modifications of MCAT-DNDC (Dai et al., 2018a) for the development of TFW-DNDC include the following considerations:

Salinity impact on plant GPP

Salinity affects plant productivity in TFFW and freshwater marshes, where surface water and soil salinities exceed the threshold of 0.5 psu and begin to stress plant physiological function (Cormier et al., 2013; Dai et al., 2018a; Krauss et al., 2009; Liu et al., 2017; Pierfelice et al., 2015). As in MCAT-DNDC (Dai et al., 2018a), daily photosynthesis in TFW-DNDC is simulated from maximum photosynthetic rate that is modified by light, vapor pressure deficit, temperature, nitrogen, soil moisture, and soil salinity. The impact of salinity on photosynthesis in MCAT-DNDC is described by a negative exponential function $f_s = e^{-\omega s}$ (Dai et al., 2018a), where ω is a coefficient, and s is salinity in psu. It should be noted that f_s is a multiplier of what photosynthesis would be in the absence of salinity. This function describes a reduction in leaf production with increasing salinity from 5–60 psu in mangroves (Dai et al., 2018a). A reduction in plant productivity (including forest height, basal area, litterfall, wood growth, root growth) with increasing soil salinity in the range 0.5–6.5 psu at our forest and oligohaline marsh sites along the two rivers was also observed from field studies (Cormier et al., 2013; Krauss et al., 2009; Liu et al., 2017; Pierfelice et al., 2015). Because there was a lack of data on photosynthesis with soil salinity along our specific transects, we assumed that the photosynthesis estimate from MCAT-DNDC is applicable to our sites, but we modified the soil salinity factor due to the lower salinity range compared with the high salinity mangrove environment. We modified the power function in MCAT-DNDC as $f_s = e^{-\omega s^2}$ to define an accelerated reduction in plant growth when salinity increased to the high end of the range from 0.5 to 10 psu predicted in our sites, especially the heavily salinity-impacted sites under drought conditions (Wang et al., 2020a). The final salinity effect on photosynthesis of the plants in freshwater wetlands with saltwater intrusion is modified as

$$f_{\text{prodsalt}} = e^{(-\omega s^2)} \text{ when } s \geq 0.5;\ f_{\text{prodsalt}} = 1 \text{ when } s < 0.5 \quad (1)$$

where f_{prodsalt} is the salinity effect on leaf production. Plant production in TFW decreases with an increase in salinity due to saltwater intrusion when salinity ≥0.5 psu.

Salinity impact on litterfall and wood growth

In MCAT-DNDC, salinity effects on mangrove litterfall and wood growth are also considered and described, when soil moisture lesser than the wilting point, by a power function: $f_{\text{mangrove}-\text{sal}} = (e^{-\omega s} + a)^b$, that is, drought can intensify the effect of salinity on mangroves. We were able to modify the salinity effects on litterfall and wood growth in TFFW. From field data collected from the forest and oligohaline marsh sites along the two rivers during 2005–2015, negative relationships between soil pore water salinity and litterfall and wood growth were observed (data not shown, but updated from Cormier et al., 2013). Therefore, salinity effects on litterfall and wood growth in TFW-DNDC during drought can be described respectively by the equations below:

$$\begin{aligned} &f_{\text{littersalt}} = -0.19s + 1.09,\ \text{when } 5.8 > s \geq 0.5; \\ &f_{\text{littersalt}} = 1 \text{ when } s \leq 0.5; \\ &f_{\text{littersalt}} = 0.02 \text{ when } s \geq 5.8 \text{ for litterfall,} \end{aligned} \quad (2)$$

$$\begin{aligned} &f_{\text{woodsalt}} = -0.20s + 1.10,\ \text{when } 5.8 > s \geq 0.5; \\ &f_{\text{woodsalt}} = 1 \text{ when } s \leq 0.5; \\ &f_{\text{woodsalt}} = 0.01 \text{ when } s \geq 5.8 \text{ for wood growth,} \end{aligned} \quad (3)$$

where $f_{\text{littersalt}}$ is the salinity effect on litter production and f_{woodsalt} is the salinity effect on wood growth.

Salinity impact on soil organic matter decomposition

Salinity affects soil organic matter decomposition in tidal wetlands including TFFW and oligohaline marshes (Luo et al., 2019; Stagg et al., 2017; Weston et al., 2011). In MCAT-DNDC, soil organic matter decomposition is affected by soil temperature and moisture, but the impact of soil salinity on decomposition is implicitly considered. Stagg et al. (2017) conducted decomposition experiments using litterbag techniques at the forest sites and oligohaline marsh sites of the Savannah and Waccamaw rivers. Litterbags of roots and rhizomes were inserted into the soil to each of three depths (10, 25, and 50 cm) and were retrieved at 0.5, 1, 3, 6, 9, and 12 months after installation. Decomposition rates (1 day^{-1}) were estimated from remaining mass over time and related to soil salinity. A negative relationship between soil salinity and decomposition rate was found and converted to a salinity limiting factor to reflect explicitly the impact of soil salinity on decomposition in TFW-DNDC using the following:

$$\begin{aligned} &f_{\text{somsalt}} = -0.0755s + 1.0377,\ \text{when } s \geq 0.5; \\ &f_{\text{somsalt}} = 1 \text{ when } s < 0.5 \end{aligned} \quad (4)$$

where f_{somsalt} is the salinity effect on soil organic matter decomposition.

Salinity and redox potential impacts on methane emissions

The rate of methane emissions is normally simulated by counting processes of methane production, consumption, and transport (plant mediated, ebullition, and diffusion). Redox potential (Eh), temperature, pH, and substrate concentrations that result from decomposition of soil organic carbon (SOC) and plant root exudation and respiration (Li et al., 2004; Yu et al., 2006; Zhang et al., 2002) as well as salinity are found to be the major factors controlling the methane production and oxidation in salinity-impacted tidal wetlands (Dai et al., 2018a). The impact of salinity on methane production in MCAT-DNDC is also described by a negative exponential function ($f_{\text{CH}_4\text{sal}} = e^{-\varphi s}$) in addition to sulfate concentration that influences CH_4 production and emission (Dai et al., 2018a), where φ is a coefficient. The relationship between methane emission and soil salinity in tidal wetlands was found to be nonlinear, and informed by past study (Poffenbarger et al., 2011; Windham-Myers et al., 2018). Over a large salinity gradient from 0 (real freshwater environment, e.g., nontidal freshwater forests) to 35 psu (marine environment, e.g., mangroves), CH_4 fluxes tend to decrease exponentially with increase salinity such that CH_4 fluxes can be negligible at very high soil salinities. However, for low salinity environment with salinity less than 10 psu (i.e., fresh, oligohaline, and mesohaline wetlands), CH_4 fluxes vary dramatically, and emissions can even increase considerably when sulfate availability is lower (Windham-Myers et al., 2018), resulting in a weak decreasing trend with salinity. Soil salinity at the lower and oligohaline marsh sites was predicted to increase as high as ~10 psu under drought conditions (Wang et al., 2020a). In this study, a weak decrease in CH_4 fluxes with increased salinity in the range 0.5–6.5 psu at our forest and oligohaline marsh sites was observed from static chamber-based flux measurements (Krauss & Whitbeck, 2012), therefore, we modified the original power function of salinity on methane fluxes in MCAT-DNDC by multiplying the original argument of the exponent by s/10 to the salinity function to reflect the slow decrease in CH_4 fluxes with salinity in the range 0.5–10 psu. The final salinity effect on methane production is described as follows:

$$f_{\mathrm{CH_4salt}} = e^{\left(\frac{-\varphi s^2}{10}\right)} \text{ when } s \geq 0.5;\ f_{\mathrm{CH_4salt}} = 1 \text{ when } s < 0.5 \quad (5)$$

where $f_{\mathrm{CH_4salt}}$ is the salinity effect on methane production and φ is a coefficient that can be calibrated to obtain its optimal value.

In MCAT-DNDC, redox potential impact on CH_4 emission was described by a negative linear relationship for mangroves with high salinities. For low salinity tidal wetlands (<5 psu) including tidal freshwater forests and oligohaline marshes, there tends to be a nonlinear inverse relationship between Eh and CH_4 fluxes (e.g., Cheng et al., 2018; Yu et al., 2006). In this study, we adopted the Eh limiting factor from Cheng et al. (2018) with a modification to the threshold of −150 to −300 mV. Field measurements of Eh from Savannah sites at 15 and 30 cm soil depths during dry (August 2006 and August 2007) and wet sampling periods (November 2006 and March 2007) showed that Eh at our sites ranged from −300 to 250 mV, and CH_4 emission tended to substantially decrease at 250 mV for tidal swamps (Yu et al., 2006). The final Eh effect on methane production (f_{E_h}) is described as follows:

$$f_{E_h} = e^{\left(-1.7\left(\frac{300+E_h}{300}\right)\right)} \text{ when } 250 > \mathrm{E_h} > -300;$$
$$f_{E_h} = 1 \text{ when } \mathrm{E_h} < -300;\ f_{E_h} = 0 \text{ when } \mathrm{E_h} > 250 \quad (6)$$

Allochthonous OC deposition from riverine sources

Krauss et al. (2018) found that carbon surface sedimentation accumulation from allochthonous riverine and autochthonous wetland sources is an important flux of carbon at TFFW sites along the two rivers, ranging from 86 to 410 g C m^{-2} $year^{-1}$. Some of the allochthonous OC from riverine sources could balance the in situ decomposition of autochthonous OC and export through erosion (Ensign et al., 2013); therefore, allochthonous carbon should be included in modeling carbon fluxes and storage. Although the percentage of allochthonous OC deposition to total OC deposition for our Waccamaw and Savannah sites was unknown, the study of Hupp et al. (2019) found that the range of allochthonous carbon deposition to total OC deposition for tidal floodplains including TFFW can be 3%–36%. A value of 3% for allochthonous vertical OC accretion was determined via model calibration in TFW-DNDC.

Input data

Input data include climate, tide, vegetation, and soil features. Site-specific information includes latitude, longitude, and elevation that were obtained from previous studies at these sites (e.g., Krauss et al., 2009; Noe et al., 2013; Stagg et al., 2016). Climate data include daily precipitation and maximum and minimum temperature. Daily temperature and rainfall at the forest and oligohaline marsh sites along the two rivers were obtained from the Oak Ridge National Laboratory's Daily Surface Weather and Climatological Summaries (Daymet) database (Thornton et al., 2020). Hydrological data include soil water level and soil pore water salinity. Daily soil water level at these TFFW sites were derived from in situ measurements of hourly water level (2004–2016) and surface elevation (Cormier et al., 2013; Krauss et al., 2009). Daily soil pore water salinity for these sites was derived from a mass balance-based hydrological model (Wang et al., 2020a and data available in Wang et al., 2020b), which in turn was calibrated using quarterly pore water measurements from TFFW sites. Vegetation data for overstory and understory layers include vegetation type; initial leaf, wood, and root mass; leaf N concentration; foliar C/N ratio; nitrogen to phosphorus ratio, and wood C/N ratio. Soil data include SOC concentration in the top soil horizon (0–5 cm), pH, bulk density, clay fraction, saturated hydrological conductivity, porosity, field capacity, wilting point, fractions of litter, and humus for both organic and mineral layers. Vegetation and soil data were obtained from previous studies at these sites (Cormier et al., 2013; Ensign et al., 2013; Jones et al., 2017; Krauss et al., 2009, 2018; Noe et al., 2013; Wang et al., 2020a) and DNDC modeling literature (Dai et al., 2018a; Li et al., 2000, 2004; Zhang et al., 2002). TFW-DNDC generates simulated carbon fluxes and storage at daily and annual intervals. TFW-DNDC outputs include GPP; NPP; plant respiration from leaf, wood, and root, soil heterotrophic respiration; SOC sequestration rate and storage. Methane and nitrous oxide are also outputs of TFW-DNDC but not included here. A formal sensitivity analysis was conducted to determine the sensitivity to model parameters for TFW-DNDC calibration. Model parameters and sensitivity analysis results can be found in Appendix S2: Table S1.

Model calibration and validation

TFW-DNDC was calibrated and validated using field measured annual litterfall, wood growth, root growth, soil respiration, and soil OC storage from previous studies (Cormier et al., 2013; Jones et al., 2017; Krauss et al., 2018; Noe et al., 2016; Stagg et al., 2017). Calibration and validation were conducted using field data on these variables from 2006 and 2007 for the Savannah River sites and from 2010 and 2011 for the Waccamaw River sites.

The performance of TFW-DNDC during calibration and validation was evaluated using the coefficient of determination (R^2). The coefficient of determination measures the linear association between the modeled and observed data; a high correlation coefficient is considered desirable, typically values greater than 0.5 are considered acceptable, and is calculated as following:

$$R^2 = \left(\frac{\sum (O_i - \overline{O})(P_i - \overline{P})}{\sqrt{(O_i - \overline{O})^2} \sqrt{(P_i - \overline{P})^2}} \right)^2 \tag{7}$$

where $\mathrm{O_i}$, $\overline{O}$, $\mathrm{P_i}$, and $\overline{P}$ are observed values, observation mean, simulated values, and simulation mean, respectively.

Scenario analysis

The calibrated and validated TFW-DNDC was used to examine the trend and variability in carbon fluxes and storage at these TFFW sites under normal and drought conditions. The normal year and dry year were selected from Wang et al. (2020a) who used the Palmer drought severity index (PDSI) for Northeast Division of South Carolina and Southeast Division of Georgia, and historical discharge data (2008–2017 for Savannah sites and 1994–2017 for Waccamaw sites). Based on Wang et al. (2020a), the years 2013 and 2012 were selected as the normal year and dry year for Waccamaw River sites, respectively (except that 2011 was used as the dry year for the middle forest site), and the years 2010 and 2012 were selected as the normal year and dry year for Savannah River sites, respectively. In situ daily soil water level data relative to soil surface at all sites and simulated daily soil pore water salinity under normal and drought conditions were used for scenario simulations. At each site, soil water level and salinity as well as climate variables varied between the normal and dry years while initial conditions of soil and vegetation were kept the same. Summary statistics of daily soil water level and soil pore water salinity for all sites are provided in Table 1, and the temporal variations of daily soil water level and soil pore water salinity are provided in Appendix S3: Figures S1 and S2.

Statistical analysis

The impacts of drought-induced saltwater intrusion and reduced soil water level on simulated carbon stock and fluxes (daily GPP, NPP, plant respiration, soil respiration, SOC sequestration, and SOC storage) at the TFFW sites along the two river systems were analyzed using a three-way ANOVA with river, site, drought, and their interaction as explanatory variables, and two-way ANOVAs with site, drought, and their interaction as explanatory variables. When necessary, the simulation results were transformed using the Box–Cox method with an optimal lambda value prior to analysis to meet normality and homoscedasticity assumptions. Whenever a significant interaction effect was detected via two-way ANOVAs, a series of one-way ANOVAs was also used to analyze individually the impact of drought on carbon stock and fluxes at each of the TFFW sites. All post hoc tests were performed using Tukey's honestly significant difference (HSD) test. The SAS 9.3 software package (SAS Institute, Cary, North Carolina, USA) was used for the statistical analyses. All the tests were two-tailed based on type III sums of squares and considered significant at $p < 0.05$.

RESULTS

The comparisons between simulated and observed annual litterfall, wood growth, root growth, soil respiration, and SOC storage showed that simulated carbon components were in good agreement with observed values ($R^2 = 0.90$ for calibration and 0.93 for validation for Waccamaw sites and $R^2 = 0.93$ for calibration and 0.92 for validation for Savannah sites) (Figure 3). Nevertheless, model performance tended to vary with sites. For example, the model tended to underestimate litterfall at the upper sites, whereas it overestimated litterfall at the middle and lower forest sites (Figure 3). Simulated SOC storage was very close to observed values with <2% relative difference for upper and middle sites

TABLE 1 Summary statistics of soil water level and soil salinity under normal and drought conditions in the upper forest, middle forest, lower forest, and oligohaline marsh sites along the Savannah River and the Waccamaw River.

	Savannah		Waccamaw	
Site	**Normal (2010)**	**Dry (2012)**	**Normal (2013)**	**Dry (2012)**
Water level (cm)				
Upper	−2.41 ± 7.62	−3.02 ± 4.55	0.46 ± 5.61	−2.34 ± 4.69
Middle	0.77 ± 6.23	−2.18 ± 6.92	3.41 ± 5.34	0.57 ± 6.24
Lower	4.64 ± 5.82	−9.88 ± 9.05	6.70 ± 5.52	6.23 ± 6.00
Marsh	10.23 ± 6.08	−0.85 ± 3.71	10.36 ± 6.01	9.93 ± 6.11
Soil salinity (psu)				
Upper	0.10 ± 0.00	0.10 ± 0.00	0.10 ± 0.00	0.10 ± 0.00
Middle	1.09 ± 0.74	2.37 ± 0.37	0.63 ± 0.57	0.78 ± 0.53
Lower	3.46 ± 2.12	7.23 ± 0.72	1.91 ± 1.14	6.45 ± 0.08
Marsh	3.63 ± 2.40	7.61 ± 1.38	2.10 ± 1.44	4.98 ± 0.38

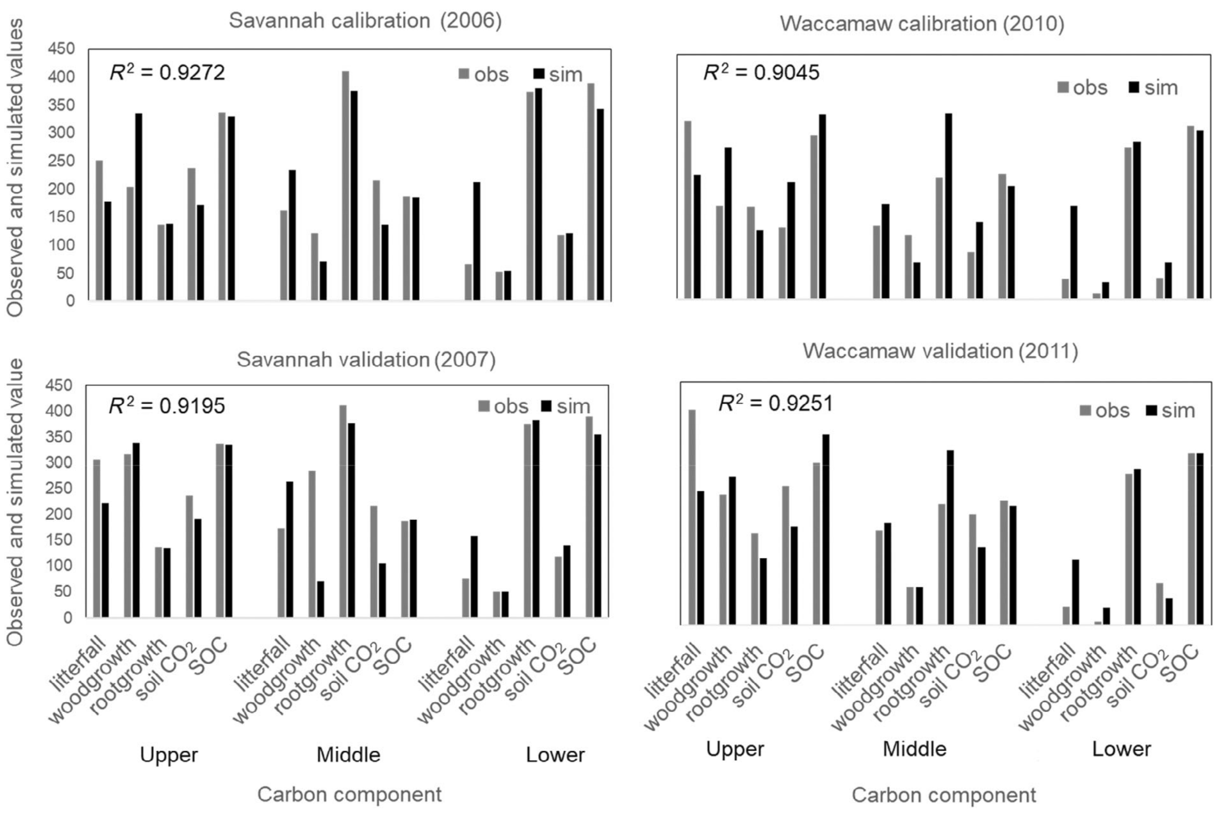

FIGURE 3 Comparison between simulated (sim) and observed (obs) carbon variables in tidal freshwater forested wetlands (TFFW) sites along the Waccamaw River and the Savannah River. SOC, soil organic carbon.

compared with −11.8% and −8.8% for calibration and validation for the lower site (Figure 3).

The three-way ANOVAs showed that there were statistically significant interactions among river, site, and drought condition on simulated soil respiration, SOC sequestration rate and SOC storage ($p < 0.0001$), but not simulated GPP ($p = 0.32$), NPP ($p = 0.43$), and plant respiration ($p = 0.10$). The two-way ANOVAs showed that there were statistically significant interactions (all, $p < 0.0001$) between site and drought condition on GPP, NPP, plant respiration, soil respiration, SOC sequestration rate, and SOC storage at Savannah River sites. For sites along Waccamaw River, there were statistically significant interactions ($p < 0.001$) between site and drought conditions on all carbon components except for SOC sequestration rate ($p = 0.58$). Therefore, a series of one-way ANOVAs was conducted to detect the statistical significance of the impacts of drought-induced saltwater intrusion on GPP, NPP, plant respiration, soil respiration, SOC sequestration rate, and SOC storage at each of the TFFW sites. The one-way ANOVAs revealed that statistically significant differences in simulated carbon components between the normal and drought conditions (data available in Wang et al., 2021) vary with sites.

Along the Savannah River, simulated GPP increased significantly in the upper forest (+174 g C m^{-2} $year^{-1}$, +50%, $p = 0.0005$) and oligohaline marsh (+127 g C m^{-2} $year^{-1}$, +49%, $p < 0.0001$) but decreased significantly in the lower forest (−158 g C m^{-2} $year^{-1}$, −51%, $p < 0.0001$) under the drought condition compared with the normal condition (Figure 4). Similarly, simulated NPP increased significantly in the upper forest (+121 g C m^{-2} $year^{-1}$, +50%, $p = 0.0005$) and marsh (+67 g C m^{-2} $year^{-1}$, +34%, $p < 0.0001$) but decreased significantly in the lower forest (−106 g C m^{-2} $year^{-1}$, −64%, $p < 0.0001$) under drought conditions (Figure 4). Simulated plant respiration increased significantly in the upper forest (+53 g C m^{-2} $year^{-1}$, +50%, $p = 0.001$), middle forest (+13 g C m^{-2} $year^{-1}$, +10%, $p = 0.009$), and oligohaline marsh (+59 g C m^{-2} $year^{-1}$, +92%, $p < 0.0001$) but decreased significantly in the lower forest (−51 g C m^{-2} $year^{-1}$, −35%, $p < 0.0001$) under the drought conditions (Figure 4).

For soil carbon pools along the Savannah River, soil respiration increased significantly in the lower forest (+139 g C m^{-2} $year^{-1}$, +120%, $p < 0.0001$) and oligohaline marsh (+46 g C m^{-2} $year^{-1}$, +148%, $p = 0.0017$) under the drought conditions compared with the normal condition (Figure 5). Simulated SOC sequestration rate decreased significantly only at the lower forest (−473 g C m^{-2} $year^{-1}$, −44%, $p < 0.0001$) under the drought conditions (Figure 5). Nevertheless, simulated SOC storage increased significantly (+4 Mg C ha^{-1}, ~2%, $p < 0.0001$) in the upper forest as a result of increased SOC sequestration rate but decreased significantly (−2~37 Mg C ha^{-1}, −1%~10%, $p < 0.0001$) in the middle forest, lower forest and

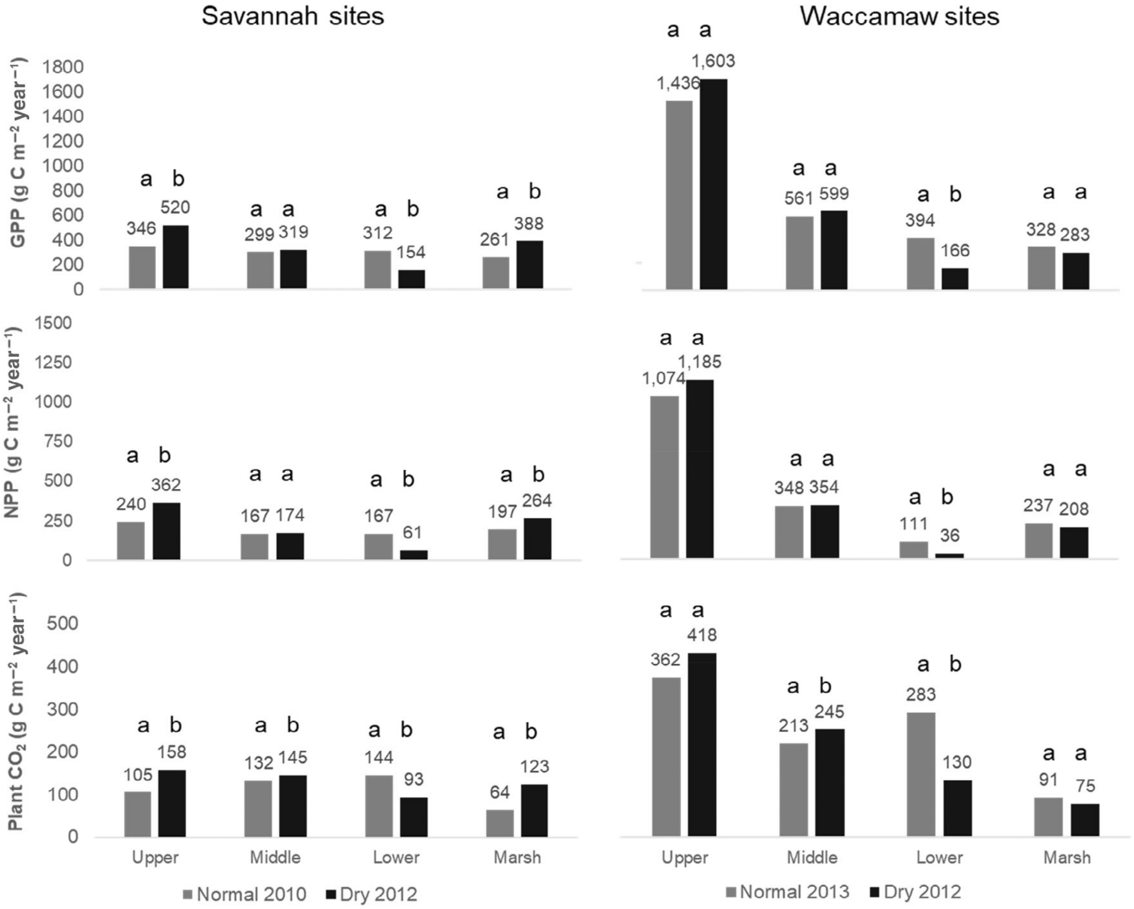

FIGURE 4 Simulated gross primary productivity (GPP), net primary productivity (NPP), and plant respiration under normal and drought conditions in tidal freshwater forested wetlands (TFFW) sites along the Waccamaw River and the Savannah River. Significant differences between the normal and drought conditions are indicated by different letters (i.e., a and b).

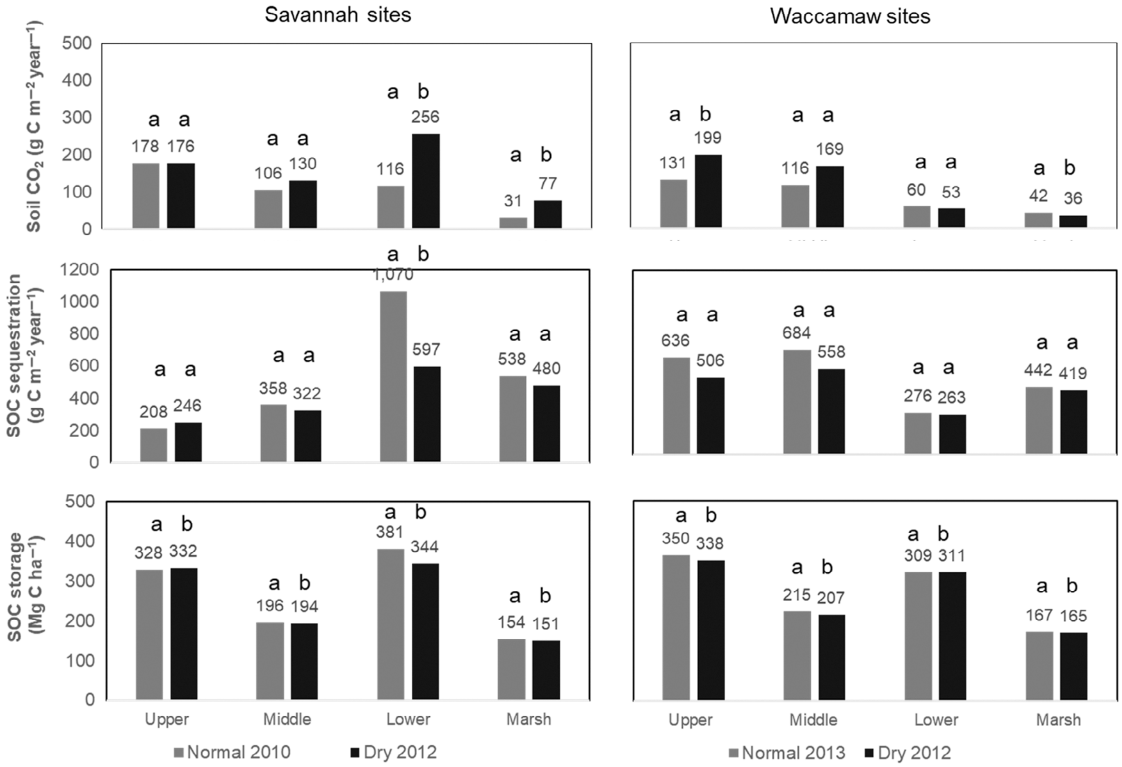

FIGURE 5 Simulated soil respiration, soil carbon sequestration and soil organic carbon (SOC) storage under normal and drought conditions in tidal freshwater forested wetlands (TFFW) sites along the Waccamaw River and the Savannah River. Significant differences between the normal and drought conditions are indicated by different letters (i.e., a and b).

oligohaline marsh due to the decline in SOC sequestration rates under the drought conditions (Figure 5).

For plant carbon pools along the Waccamaw River, simulated GPP and NPP decreased significantly ($p < 0.0001$) only in the lower forest under the drought conditions with increased soil salinity and reduced soil water level. The simulated values decreased by 229 and 68 g C m^{-2} year^{-1} for GPP and NPP (−58% and −75%), respectively, under the drought conditions compared with the normal conditions (Figure 4). Simulated plant respiration increased significantly (+32 g C m^{-2} year^{-1}, +15%, $p = 0.0049$) in the middle forest but decreased significantly (−50%, −153 g C m^{-2} year^{-1}, $p < 0.0001$) in the lower forest under the drought conditions (Figure 4).

For soil carbon pools along the Waccamaw River, unlike the Savannah River, simulated soil respiration increased significantly in the upper forest (+67 g C m^{-2} year^{-1}, +51%, $p = 0.0454$) but decreased significantly in the oligohaline marsh (−6 g C m^{-2} year^{-1}, −15%, $p < 0.0001$) under the drought conditions (Figure 5). Simulated SOC sequestration rate did not show significant changes ($p = 0.1637 \sim 0.7496$) although the trend of decreasing SOC by 12–129 g C m^{-2} year^{-1} at all four sites under the drought conditions was noteworthy (Figure 5). Despite the statistically insignificant changes in SOC sequestration rate in soils along the Waccamaw River, simulated SOC storage showed significant changes ($p < 0.0001$) under the drought conditions. The simulated SOC storage decreased by 12 Mg C ha^{-1} (3%), 9 Mg C ha^{-1} (4%), and 2 Mg C ha^{-1} (1%) in the upper forest, middle forest, and oligohaline marsh, respectively, whereas SOC increased by 2 Mg C ha^{-1} (<0.5%) in the lower forest (Figure 5).

DISCUSSION

Our first key finding is that responses of GPP and NPP in TFFW to drought-induced saltwater intrusion vary by river system and individual site. GPP and NPP in the lower forest along the two rivers were significantly lower under drought conditions and this decline can be attributed to increased salinity stress. Under the drought conditions, simulated soil salinities were in the range 6.4–6.7 psu on Waccamaw lower and 5.5 to 9.9 psu on Savannah lower, much higher than the concentration (<2 psu) under typical TFFW-maintaining conditions (Table 1). Specifically, reduction of NPP under the drought conditions was due to the decline in litterfall (−37%∼−63%) and wood growth (as high as −19%) rather than a decline in root growth in the two lower forests (data not shown). Root growth increased by 6% and 18% in Savannah lower forest and Waccamaw lower forest under the drought conditions. Litterfall was found to make up 63% of total aboveground NPP (ANPP), whereas stem wood growth contributed 37% in TFFW of northeastern South Carolina (Ozalp et al., 2007). Previous TFFW productivity studies also showed that increased salinity reduced average ANPP due to the decline in average stem wood growth and litterfall (e.g., Cormier et al., 2013; Pierfelice et al., 2015), whereas belowground NPP (BNPP) did generally increase (From et al., 2021), as it did in our simulated drought.

In contrast, GPP and NPP slightly increased in the upper forest along the two rivers under the drought conditions, suggesting that extended hydroperiod is the major limiting factor controlling plant growth in the continuously freshwater upper forest. GPP and NPP in Savannah upper forest were lower than Waccamaw upper forest under both normal and drought conditions, which could be attributed to the relatively lower supply of N in the alluvial Savannah River (Noe et al., 2013; Ozalp et al., 2007). For the lower forest sites, GPP and NPP could be salinity or hydrology limited. Thomas et al. (2015) found that tree growth at Savannah middle showed a strong negative correlation with river salinity, whereas tree growth at Waccamaw middle did not relate as much to salinity as Savannah middle. Opposite responses of GPP and NPP under the drought conditions in the oligohaline marshes along the two rivers were revealed in TFW-DNDC simulations; significant increases of GPP and NPP with drought in Savannah marsh contrasted with no significant change in Waccamaw marsh (but with decreasing trend). The increase in GPP and NPP at Savannah oligohaline marsh site with drought was due to the large reduction in soil average water level or moisture state, and the no change in GPP and NPP at Waccamaw oligohaline marsh sites is because water level was still relatively high with drought (Table 1). Therefore, the differential response is due to removal or not of inundation stress.

The different responses of tree growth to increasing salinity in our simulations and previous studies indicated that there could be tipping points or thresholds in soil salinity and water level that determined state changes in plant community composition and productivity in TFFW. Furthermore, these tipping points would depend on the combination of hydrology and salinity regimes interactively with nutrient (N and P) regimes (Krauss et al., 2009; Noe et al., 2013). Baldcypress growth was found to be restricted by salinity below 6 psu under acute salinity stress in experimental settings and below 2–4 psu for chronically imposed salinity in the field (Duberstein et al., 2020; Krauss & Duberstein, 2010). When salinity was at 2–5 psu, salinity stress thresholds of both freshwater woody and herbaceous plants may replace flood tolerance in controlling plant community composition, growth, and related soil biogeochemical processes, whereas the salt-tolerant oligohaline marsh species appear to be less influenced by increased salinity during drought and instead benefit from reduced hydroperiod during drought conditions (Krauss et al., 2009; Noe et al., 2013).

Our second key finding is that the responses of plants including belowground live root and soil heterotrophic respiration in TFFW to drought-induced saltwater intrusion also vary by river system and tidal wetland type. The increase in plant respiration in upper forests (true freshwater forest) and middle forests (less salinity impacted) under the drought conditions along the two rivers could be attributed to increased root respiration with the reduction of water table depth because root respiration in TFFW was found to be inhibited primarily by flooding (Krauss & Whitbeck, 2012). In contrast, the decrease in plant respiration in the high salinity lower forest sites along both rivers may primarily be the result of salinity inhibition on belowground root respiration (Krauss et al., 2012). This outcome indicates that salinity stress exerts a more important influence than soil water level in regulating plant respiration when TFFW begin to experience oligohaline conditions. The significant increase in plant respiration in the Savannah marsh under drought, conversely, is likely to be the result of the significant drop (>108%; Table 1) in soil water table.

A significant increase in soil respiration under the drought conditions in the Savannah lower forest and oligohaline marsh and in the Waccamaw upper forest in comparison with a significant decrease in soil respiration in the Waccamaw oligohaline marsh indicates that potential soil organic matter decomposition and mineralization in low salinity wetlands have a complexity dependent on their very specific geographic locations, an observation also described by others (Luo et al., 2019; Marton et al., 2012; Weston et al., 2011). For instance, Marton et al. (2012) observed significantly increased soil CO_2 emission for tidal forest soils collected along the Altamaha River and treated with salinities of 2 and 5 psu compared with a 0 psu control. However, this result was not consistent, with tidal forest soils collected along the Satilla and Ogeechee rivers and subjected to the same experimental design, despite the location of all rivers along the coast of Georgia, USA. The different responses of soil respiration in TFFW reflected the combined effects of soil salinity and soil water table on soil organic matter decomposition and plant primary production that stimulate root growth and regulate respiration belowground. Reduction in soil water level alone may cause increased soil respiration (Spivak et al., 2019), whereas increases in soil salinity alone may result in reduced soil respiration due to the negative effect on microbial communities, decreases in microbial activity (Chambers et al., 2013), and reductions of plant primary productivity (Mueller et al., 2016). Greater amounts of microbially released CO_2 could be found under both acute salinity incursion and efficient SOC oxidation (Weston et al., 2006). The increase in soil respiration in the salinity-affected middle forest, lower forest and oligohaline marshes along the Savannah River under drought conditions could be explained by the introduction of abundant SO_4^{-2} from saltwater intrusion that served as an electron acceptor without inhibiting microbial activities through ionic or osmotic stress (Luo et al., 2019). The significantly increased soil respiration under the drought conditions in the Waccamaw upper forest where soil salinity was not affected (<0.5 psu) was primarily the result of lower soil water level rather than changes in soil salinity (Krauss et al., 2012; Liu et al., 2017), resulting in the enhanced organic matter decomposition during drought. Overall, the net outcomes of soil respiration in response to drought-induced saltwater intrusion were not simply the addition of salinity and hydrology effects, which can be mutually enhancing in some cases but mutually inhibiting in other cases (Luo et al., 2019). This complexity is captured by TFW-DNDC, but will be refined further in time to apply to a wider range of TFFW and oligohaline transitions.

Our third key finding is that because of the decreasing SOC sequestration rate, especially at Savannah lower forest under drought-induced saltwater intrusion, simulated SOC storage under drought conditions decreased significantly at TFFW sites (i.e., six out of the eight sites had decreased SOC). SOC decrease was as high as −10% in the Savannah lower forest, and TFW-DNDC projected only a slight increase of <1% at other two sites (Savannah upper forest and Waccamaw lower forest). The decrease in SOC sequestration and storage under drought conditions can be attributed to increased microbial oxidation of soil organic matter with the switch from anaerobic to aerobic soil status, especially during warm periods in late spring through summer when the process of microbial decomposition of organic matter is further stimulated (Spivak et al., 2019). SOC storage was found to decrease significantly from stimulated microbial decomposition in tidal freshwater marsh soils experiencing saltwater intrusion in a year-long laboratory experiment in which intact soils were exposed to ∼5 psu salinity for the first time (Weston et al., 2011). As with the salinity stress for plant production, our modeling results also suggest that there should be salinity thresholds for detecting the directional changes (increase, no change, or decrease) in soil respiration, SOC sequestration, and carbon storage.

Drought-induced saltwater intrusion results in a large increase in soil pore water salinity (Wang et al., 2020a). Under future climate change-induced drought conditions, upper and middle forests along the two rivers are likely to be converting to lower forest and to oligohaline marsh types (0.5–5 psu), and in time might change to mesohaline marshes (5–18 psu) or unvegetated open water, depending on the severity and duration of drought-induced salinity intrusion. Jones et al. (2017) found that the oligohaline marshes along the two rivers transitioned from TFFW between 300–500 years ago with rising sea levels and colonial land clearance. If these upper and middle forests change to lower forest types under long-term (decadal or centurial) climate change and SLR, large decreases in plant productivity (GPP/NPP), SOC sequestration rate, and significant losses of carbon that has been stored over centuries from TFFW as a whole can be anticipated, therefore reducing the capacity of TFFW as carbon sinks and decreasing the resilience to increased relative SLR (Jones et al., 2017; Stagg et al., 2016). Among the modeled carbon fluxes, NPP and SOC sequestration rate are the two fluxes that have consistent and large relative magnitude of change in both Savannah and Waccamaw lower forest sites under drought-induced saltwater intrusion compared with the normal conditions. NPP could decrease by −64% and −68% and SOC sequestration rates decrease by −44% and −4% in the Savannah and Waccamaw lower forest sites, respectively, with repetitive future droughts. These reductions in NPP and SOC sequestration rate are large enough to have an impact on the role of the upper tidal estuary in mediating blue carbon flux and storage.

Krauss et al. (2018) defined carbon mass balance as the differences between the sum of inputs (litterfall, wood/stem growth, root growth, and surface sediment accumulation) and sum of outputs (surface litter decomposition, root decomposition, and GHG fluxes from root respiration and plant transport). Relative to these mass balance data, we find two things. First, the decreases in NPP under drought conditions accounted for more than 17% of the carbon mass balance in salt-impacted transitional forests along the Savannah ($4\ \mathrm{km}^2$, mass balance = $2.4 \pm 1.0\ \mathrm{Gg\ C\ year}^{-1}$) and Waccamaw ($31.7\ \mathrm{km}^2$, $13.9 \pm 6.5\ \mathrm{Gg\ C\ year}^{-1}$) rivers. Second, the decreases in SOC sequestration rate under drought conditions accounted for ∼270% of the soil carbon burial of the salt-impacted transitional forest in Savannah River ($0.7 \pm 0.6\ \mathrm{Gg\ C\ year}^{-1}$) and ∼20% of the carbon burial in Waccamaw River ($0.5 \pm 0.1\ \mathrm{Gg\ C\ year}^{-1}$). At a larger geographical gradient, assuming existing $1916\ \mathrm{km}^2$ tidal freshwater forest along the Atlantic coast (Windham-Myers et al., 2018) were converted to lower forest type under climate change and SLR, using the SOC sequestration loss rate ($-473\ \mathrm{g\ C\ m}^{-2}\ \mathrm{year}^{-1}$) from the Savannah lower forest, it is estimated that SOC from the tidal freshwater forest along the Atlantic coast could be lost to droughts at 0.95 Tg C per year. The loss could be 3.4% of carbon sequestration of total wetlands in North America (27 ± 13 Tg C per year from the atmosphere) and 16.5% of total riverine and tidal wetland input into estuaries along the Atlantic coast (Windham-Myers et al., 2018). Our results showed that the magnitude and direction of changes in GPP, NPP, plant and soil respiration, soil carbon sequestration, and storage in TFFW vary greatly with site-specific soil salinity and water level conditions, implying that there are large uncertainties in TFFW blue carbon accounting and assessment.

Ecosystem based management implementations to restore TFFW hydrologic connectivity with the freshwater and saltwater tidal balance, as well as implementing measures to control surface and soil water salinity, may be needed in the future. Depending on specific local hydrological conditions, engineering measures such as river diversions, strategic breaching of former rice fields, or saltwater control system might be required to maintain or enhance TFFW carbon sequestration capacity as SLR continues to impact and water extraction continues from up-river dams. For example, it was found that in the lower Mississippi River, intermediate discharge from freshwater river re-introduction projects (diversions) could not only bring freshwater and mineral sediment to sediment starved wetlands to control salinity and rebuild wetlands, but also enhance SOC sequestration (Wang et al., 2017). Because the reduction of freshwater supply is inevitable under climate change-induced drought conditions and greater up-river water extraction for consumptive use, future TFFW management actions could avoid flooding of water with elevated salinity and draining wetlands during growing seasons and maintaining tidal flooding, if carbon sequestration and storage are to be maintained or enhanced (Drexler et al., 2013).

ACKNOWLEDGMENTS

This research was supported by the United States Geological Survey (USGS) Climate Research and Development Program, USGS Ecosystems Mission Area, and NASA Carbon Monitoring Systems Program (#80HQTR18T0012) to the United States Department of Agriculture Forest Service. We would like to thank Andy S. From, Nicole Cormier, Rebecca F. Moss, and Miriam Jones for their assistance in field data collection and analysis. We thank Michael J. Osland and two anonymous reviewers for their constructive review that improved this manuscript. Any use of trade, firm, or product names is for descriptive purposes only and does not imply endorsement by the United States Government.

CONFLICT OF INTEREST

The authors declare no conflict of interest.

DATA AVAILABILITY STATEMENT

Data sets utilized for this research are available from the Oak Ridge National Laboratory and USGS ScienceBase as follows: Thornton et al. (2020) (https://doi.org/10.3334/ORNLDAAC/1840); Wang et al. (2020b) (https://doi.org/10.5066/P9JVZZ4N); Wang et al. (2021) (https://doi.org/10.5066/P98R3ZXE).

ORCID

Hongqing Wang https://orcid.org/0000-0002-2977-7732
Zhaohua Dai https://orcid.org/0000-0002-0941-8345
Carl C. Trettin https://orcid.org/0000-0003-0279-7191
Ken W. Krauss https://orcid.org/0000-0003-2195-0729
Gregory B. Noe https://orcid.org/0000-0002-6661-2646
Andrew J. Burton https://orcid.org/0000-0002-3068-0997
Camille L. Stagg https://orcid.org/0000-0002-1125-7253
Eric J. Ward https://orcid.org/0000-0002-5047-5464

REFERENCES

Chambers, L. G., T. Z. Osborne, and K. R. Reddy. 2013. "Effect of Salinity-Altering Pulsing Events on Soil Organic Carbon Loss along an Intertidal Wetland Gradient: A Laboratory Experiment." *Biogeochemistry* 115: 363–83.

Cheng, Y., C. Tong, D. Du, L. Tan, H. Li, and Q. Rao. 2018. "Modelling the Diurnal Variations of Methane Emissions from the *Cyperus malaccensis* Tidal Marsh in the Minjiang River Estuary." *Wetlands* 38: 293–305.

Conner, W. H., J. A. Duberstein, J. W. Day, and S. Hutchinson. 2014. "Impacts of Changing Hydrology and Hurricanes on Forest Structure and Growth along a Flooding/Elevation Gradient in a South Louisianan Forested Wetland from 1986 to 2009." *Wetlands* 34: 803–14.

Cormier, N., K. W. Krauss, and W. H. Conner. 2013. "Periodicity in Stem Growth and Litterfall in Tidal Freshwater Forested Wetlands: Influence of Salinity and Drought on Nitrogen Recycling." *Estuaries and Coasts* 36: 533–46.

Dai, Z., C. C. Trettin, S. Frolking, and R. A. Birdsey. 2018a. "Mangrove Carbon Assessment Tool: Model Development and Sensitivity Analysis." *Estuarine, Coastal and Shelf Science* 208: 23–35.

Dai, Z., C. C. Trettin, S. Frolking, and R. A. Birdsey. 2018b. "Mangrove Carbon Assessment Tool: Model Validation and Assessment of Mangroves in Southern USA and Mexico." *Estuarine, Coastal and Shelf Science* 208: 107–17.

Drexler, J. Z., K. W. Krauss, M. C. Sasser, C. C. Fuller, C. M. Swarzenski, A. Powell, K. M. Swanson, and J. Orlando. 2013. "A Long-Term Comparison of Carbon Sequestration Rates in Impounded and Naturally Tidal Freshwater Marshes along the Lower Waccamaw River, South Carolina." *Wetlands* 33: 965–74.

Duberstein, J. A., K. W. Krauss, M. J. Baldwin, S. T. Allenc, W. H. Conner, J. S. SalterJr, and M. Miloshis. 2020. "Small

Gradients in Salinity Have Large Effects on Stand Water Use in Freshwater Wetland Forests." *Forest Ecology and Management* 473: 118308.

Ensign, S. H., C. R. Hupp, G. B. Noe, K. W. Krauss, and C. L. Stagg. 2013. "Sediment Accretion in Tidal Freshwater Forests and Oligohaline Marshes of the Waccamaw and Savannah Rivers, USA." *Estuaries and Coasts* 37: 1107–19.

From, A. S., K. W. Krauss, G. B. Noe, N. Cormier, C. L. Stagg, R. F. Moss, and J. L. Whitbeck. 2021. "Belowground Productivity Varies by Technique and Vegetation Type in Tidal Freshwater Forested Wetlands Transitioning to Marsh." *PLoS One* 16: e0253554. https://doi.org/10.1371/journal.pone.0253554.

Hackney, C. T., G. B. Avery, L. A. Leonard, M. Posey, and T. Alphin. 2007. "Biological, Chemical, and Physical Characteristics of Tidal Freshwater Swamp Forests of the Lower Cape Fear River/Estuary, North Carolina." In *Ecology of Tidal Freshwater Forested Wetlands of the Southeastern United States*, edited by W. H. Conner, T. W. Doyle, and K. W. Krauss, 183–221. New York: Springer.

Hupp, C. R., D. E. Kroes, G. B. Noe, E. R. Schenk, and R. H. Day. 2019. "Sediment Trapping and Carbon Sequestration in Floodplains of the Lower Atchafalaya Basin, LA: Allochthonous Versus Autochthonous Carbon Sources." *Journal of Geophysical Research: Biogeosciences* 124: 663–77.

Jones, M. C., C. E. Bernhardt, K. W. Krauss, and G. B. Noe. 2017. "The Impact of Late Holocene Land Use Change, Climate Variability, and Sea Level Rise on Carbon Storage in Tidal Freshwater Wetlands on the Southeastern United States Coastal Plain." *Journal of Geophysical Research: Biogeosciences* 122: 3126–41.

Korol, A. R., and G. B. Noe. 2020. "Patterns of Denitrification Potential in Tidal Freshwater Forested Wetlands." *Estuaries and Coasts* 43: 329–46.

Krauss, K. W., and J. A. Duberstein. 2010. "Sapflow and Water Use of Freshwater Wetland Trees Exposed to Saltwater Incursion in a Tidally Influenced South Carolina Watershed." *Canadian Journal of Forest Research* 40: 525–35.

Krauss, K. W., J. A. Duberstein, T. W. Doyle, W. H. Conner, R. H. Day, L. W. Inabinette, and J. L. Whitbeck. 2009. "Site Condition, Structure, and Growth of Baldcypress along Tidal/Non-tidal Salinity Gradients." *Wetlands* 29: 505–19.

Krauss, K. W., G. B. Noe, J. A. Duberstein, W. H. Conner, C. L. Stagg, N. Cormier, M. C. Jones, et al. 2018. "The Role of the Upper Tidal Estuary in Wetland Blue Carbon Storage and Flux." *Global Biogeochemical Cycles* 32: 817–39.

Krauss, K. W., and J. L. Whitbeck. 2012. "Soil Greenhouse Gas Fluxes during Wetland Forest Retreat along the Lower Savannah River, Georgia (USA)." *Wetlands* 32: 73–81.

Krauss, K. W., J. L. Whitbeck, and R. J. Howard. 2012. "On the Relative Roles of Hydrology, Salinity, Temperature, and Root Productivity in Controlling Soil Respiration from Coastal Swamps (Freshwater)." *Plant and Soil* 358: 265–74.

Li, C., J. Aber, F. Stange, K. Butgtger-Bahl, and H. Papen. 2000. "A Process-Oriented Model of N_2O and NO Emissions from Forest Soils. I. Model Development." *Journal of Geophysical Research: Atmospheres* 105: 4369–84.

Li, C., J. Cui, G. Sun, and C. Trettin. 2004. "Modeling Impacts of Management on Carbon Sequestration and Trace Gas Emissions in Forested Wetland Ecosystems." *Environmental Management* 33: S176–86.

Liu, X. J., A. Ruecker, B. Song, J. Xing, W. H. Conner, and A. T. Chow. 2017. "Effects of Salinity and Wet-Dry Treatments on C and N Dynamics in Coastal-Forested Wetland." *Soil Biology and Biochemistry* 112: 56–67.

Lovelock, C. E., and C. M. Duarte. 2019. "Dimensions of Blue Carbon and Emerging Perspectives." *Biology Letters* 15: 20180781.

Luo, M., J. Huang, W. Zhu, and C. Tong. 2019. "Impacts of Increasing Salinity and Inundation on Rates and Pathways of Organic Carbon Mineralization in Tidal Wetlands: A Review." *Hydrobiologia* 827: 31–49.

Marton, J. M., E. R. Hervert, and C. B. Craft. 2012. "Effects of Salinity on Denitrification and Greenhouse Gas Production from Laboratory-Incubated Tidal Forest Soils." *Wetlands* 32: 347–57.

Mueller, P., K. Jensen, and J. P. Megonigal. 2016. "Plants Mediate Soil Organic Matter Decomposition in Response to Sea Level Rise." *Global Change Biology* 22: 404–14.

Neubauer, S. C., R. B. Franklin, and D. J. Berrier. 2013. "Saltwater Intrusion into Tidal Freshwater Marshes Alters the Biogeochemical Processing of Organic Carbon." *Biogeosciences* 10: 8171–83.

Noe, G. B., C. R. Hupp, C. E. Bernhardt, and K. W. Krauss. 2016. "Contemporary Deposition and Long-Term Accumulation of Sediment and Nutrients by Tidal Freshwater Forested Wetlands Impacted by Sea Level Rise." *Estuaries and Coasts* 39: 1006–19.

Noe, G. B., K. W. Krauss, B. G. Lockaby, W. Conner, and C. R. Hupp. 2013. "The Effect of Increasing Salinity and Forest Mortality on Soil Nitrogen and Phosphorus Mineralization in Tidal Freshwater Forested Wetlands." *Biogeochemistry* 114: 225–44.

Ozalp, M., W. H. Conner, and B. G. Lockaby. 2007. "Above-Ground Productivity and Litter Decomposition in a Tidal Freshwater Forested Wetland on Bull Island, SC, USA." *Forest Ecology and Management* 245: 31–43.

Pierfelice, K. N., B. G. Lockaby, K. W. Krauss, W. H. Conner, G. B. Noe, and M. C. Ricker. 2015. "Salinity Influences on Aboveground and Belowground Net Primary Productivity in Tidal Wetlands." *Journal of Hydrologic Engineering* 22: D5015002.

Poffenbarger, H. J., B. A. Needelman, and J. P. Megonigal. 2011. "Salinity Influence on Methane Emissions from Tidal Marshes." *Wetlands* 31: 831–42.

Spivak, A. C., J. Sanderman, J. L. Bowen, E. A. Canuel, and C. S. Hopkinson. 2019. "Global-Change Controls on Soil-Carbon Accumulation and Loss in Coastal Vegetated Ecosystems." *Nature Geoscience* 12: 685–962.

Stagg, C. L., K. W. Krauss, D. R. Cahoon, N. Cormier, W. H. Conner, and C. M. Swarzenski. 2016. "Processes Contributing to Resilience of Coastal Wetlands to Sea-Level Rise." *Ecosystems* 19: 1445–59.

Stagg, C. L., D. R. Schoolmaster, K. W. Krauss, N. Cormier, and W. H. Conner. 2017. "Causal Mechanisms of Soil Organic Matter Decomposition: Deconstructing Salinity and Flooding Impacts in Coastal Wetlands." *Ecology* 98: 2003–18.

Thomas, B. L., T. W. Doyle, and K. W. Krauss. 2015. "Annual Growth Patterns of Baldcypress (*Taxodium distichum*) along Salinity Gradients." *Wetlands* 35: 831–939.

Thornton, M. M., R. Shrestha, Y. Wei, P. E. Thornton, S. Kao, and B. E. Wilson. 2020. “Daymet: Daily Surface Weather Data on a 1-km Grid for North America, Version 4.” Oak Ridge, TN: ORNL DAAC. https://doi.org/10.3334/ORNLDAAC/1840.

Wang, H., Z. Dai, C. C. Trettin, K. W. Krauss, G. B. Noe, A. J. Burton, C. L. Stagg, and E. J. Ward. 2021. “Modeling Impacts of Drought-Induced Salinity Intrusion on Carbon Fluxes and Storage in Tidal Freshwater Forested Wetlands.” U.S. Geological Survey. https://doi.org/10.5066/P98R3ZXE.

Wang, H., K. W. Krauss, G. B. Noe, C. L. Stagg, C. M. Swarzenski, J. A. Duberstein, W. H. Conner, and D. L. DeAngelis. 2020a. “Modeling Soil Porewater Salinity Response to Drought in Tidal Freshwater Forested Wetlands.” *Journal of Geophysical Research: Biogeosciences* 125(2): e2018JG004996.

Wang, H., K. W. Krauss, G. B. Noe, C. L. Stagg, C. M. Swarzenski, J. A. Duberstein, W. H. Conner, and D. L. DeAngelis. 2020b. “Modeling Soil Pore Water Salinity Response to Drought in Tidal Freshwater Forested Wetlands.” U.S. Geological Survey. https://doi.org/10.5066/P9JVZZ4N.

Wang, H., G. D. Steyer, B. R. Couvillion, H. J. Beck, J. M. Rybczyk, V. H. Rivera-Monroy, K. W. Krauss, and J. M. Visser. 2017. “Predicting Landscape Effects of Mississippi River Diversions on Soil Organic Carbon Sequestration.” *Ecosphere* 8: e01984.

Weston, N. B., R. E. Dixon, and S. B. Joye. 2006. “Ramifications of Increased Salinity in Tidal Freshwater Sediments: Geochemistry and Microbial Pathways of Organic Matter Mineralization.” *Journal of Geophysical Research: Biogeosciences* 111: G01009.

Weston, N. B., M. A. Vile, S. C. Neubauer, and D. J. Velinsky. 2011. “Accelerated Microbial Organic Matter Mineralization Following Salt-Water Intrusion into Tidal Freshwater Marsh Soils.” *Biogeochemistry* 102: 135–51.

Windham-Myers, L., W.-J. Cai, S. R. Alin, A. Andersson, J. Crosswell, K. H. Dunton, J. M. Hernandez-Ayon, et al. 2018. “Tidal Wetlands and Estuaries.” In *Second State of the Carbon Cycle Report (SOCCR2): A Sustained Assessment Report*, edited by N. Cavallaro, G. Shrestha, R. Birdsey, M. A. Mayes, R. G. Najjar, S. C. Reed, P. Romero-Lankao, and Z. Zhu, 596–648. Washington, DC: U.S. Global Change Research Program. https://doi.org/10.7930/SOCCR2.2018.Ch15.

Yu, K., S. P. Faulkner, and W. H. Patrick, Jr. 2006. “Redox Potential Characterization and Soil Greenhouse Gas Concentration across a Hydrological Gradient in a Gulf Coast Forest.” *Chemosphere* 62: 905–14.

Zhang, Y., C. Li, C. C. Trettin, H. Li, and G. Sun. 2002. “An Integrated Model of Soil, Hydrology, and Vegetation for Carbon Dynamics in Wetland Ecosystems.” *Global Biogeochemical Cycles* 16: 1061.

SUPPORTING INFORMATION

Additional supporting information can be found online in the Supporting Information section at the end of this article.

How to cite this article: Wang, Hongqing, Zhaohua Dai, Carl C. Trettin, Ken W. Krauss, Gregory B. Noe, Andrew J. Burton, Camille L. Stagg, and Eric J. Ward. 2022. “Modeling Impacts of Drought-Induced Salinity Intrusion on Carbon Dynamics in Tidal Freshwater Forested Wetlands.” *Ecological Applications* e2700. https://doi.org/10.1002/eap.2700